Reactive and nonreactive scattering of N-2 from Ru(0001): A six-dimensional adiabatic study

Diaz, C.; Vincent, J.K.; Krishnamohan, G.P.; Olsen, R.A.; Kroes, G.J.; Honkala, Johanna Karoliina; Nørskov, Jens Kehlet

Published in:
Journal of Chemical Physics

Link to article, DOI:
10.1063/1.2229197

Publication date:
2006

Document Version
Publisher's PDF, also known as Version of record

Reactive and nonreactive scattering of N_2 from Ru(0001): A six-dimensional adiabatic study

C. Díaz,[a] J. K. Vincent,[b] G. P. Krishnamohan, R. A. Olsen, and G. J. Kroes
Leiden Institute of Chemistry, Gorlaeus Laboratories, Leiden University, P.O. Box 9502, 2300 RA Leiden, The Netherlands

K. Honkala[c] and J. K. Nørskov
Center for Atomic-scale Materials Physics, Department of Physics, NanoDTU, Technical University of Denmark, DK-2800 Lyngby, Denmark

(Received 11 April 2006; accepted 22 June 2006; published online 19 September 2006)

We have studied the dissociative chemisorption and scattering of N_2 on and from Ru(0001), using a six-dimensional quasiclassical trajectory method. The potential energy surface, which depends on all the molecular degrees of freedom, has been built applying a modified Shepard interpolation method to a data set of results from density functional theory, employing the RPBE generalized gradient approximation. The frozen surface and Born-Oppenheimer [Ann. Phys. (Leipzig) **84**, 457 (1927)] approximations were used, neglecting phonons and electron-hole pair excitations. Dissociative chemisorption probabilities are found to be very small even for translational energies much higher than the minimum reaction barrier, in good agreement with experiment. A comparison to previous low dimensional calculations shows the importance of taking into account the multidimensional effects of N_2 rotation and translation parallel to the surface. The new calculations strongly suggest a much smaller role of nonadiabatic effects than previously assumed on the basis of a comparison between low dimensional results and experiments [J. Chem. Phys. **115**, 9028 (2001)]. Also in agreement with experiment, our theoretical results show a strong dependence of reaction on the initial vibrational state. Computed angular scattering distributions and parallel translation energy distributions are in good agreement with experiments on scattering, but the theory overestimates vibrational and rotational excitations in scattering. © *2006 American Institute of Physics*. [DOI: 10.1063/1.2229197]

I. INTRODUCTION

The surface science community has taken a strong interest in the N_2/Ru(0001) system during the last few decades, due to the fact that ruthenium is considered a good candidate for replacing iron as a catalyst in the industrial synthesis of ammonia, and because dissociation of N_2 is the rate-limiting step in this process. As a consequence of this interest a large number of experimental[1–13] and theoretical[5,11,14] studies have been published, showing unusual and sometimes controversial results. Although recent theoretical and experimental work[15–17] has proved that dissociation at Ru steps is much more efficient than at the Ru(0001) terraces, N_2/Ru(0001) is of much fundamental interest. This system can be considered as a new prototype system for activated dissociative chemisorption, because it exhibits properties quite different from the well studied H_2/Cu (Ref. 18) system. For instance, the minimum reaction barrier (V^*) is located further in the exit channel for N_2/Ru(0001) ($r_b \approx r_e + 1.3a_0$) (Ref. 7) than for H_2/Cu ($r_b \approx r_e + 0.8a_0$),[19] and its height is much larger for N_2/Ru(0001) (around 2 eV)[4] than for H_2/Cu (around 0.5 eV).[19]

One of the most striking features of the N_2/Ru(0001) system is that the measured reaction probability (S_0) increases very slowly with the incidence energy (E_i) for energies above the minimum reaction barrier and saturates at a very small value (10^{-2}) for $E_i \gg V^*$. Experimentally, it has also been found that the dissociation probability shows a very strong dependence on the initial vibrational state, vibrational energy being more efficient at promoting reaction than translational energy[4] (see also Fig. 1 of Ref. 9). Isotope effects have also been investigated.[6] No isotope effect has been observed in the classical regime ($E_i \geqslant V^*$), but for lower energies the reaction probability for $^{15}N_2$ is smaller than for $^{14}N_2$, which has been interpreted in terms of tunneling through a large barrier for dissociation.[6] Another unexpected feature is the lack of vibrational excitation in molecular-beam experiments for N_2 scattering from Ru(0001),[13] and the small amount of vibrational excitation observed in laser assisted associative desorption (LAAD),[11] associative desorption being the reverse process to dissociative chemisorption. Late barrier systems (reaction barrier found for an extended vibrational coordinate) are expected to exhibit significant vibrational excitation of the molecule upon scat-

[a]Electronic mail: c.diaz@chem.leidenuniv.nl
[b]Present address: Department of Physical Chemistry, Uppsala University, Box 579, S-7123 Uppsala, Sweden.
[c]Present address: Nanoscience Center, Department of Physics, University of Jyväskylä, P.O. Box 35, FIN-40014, Finland.

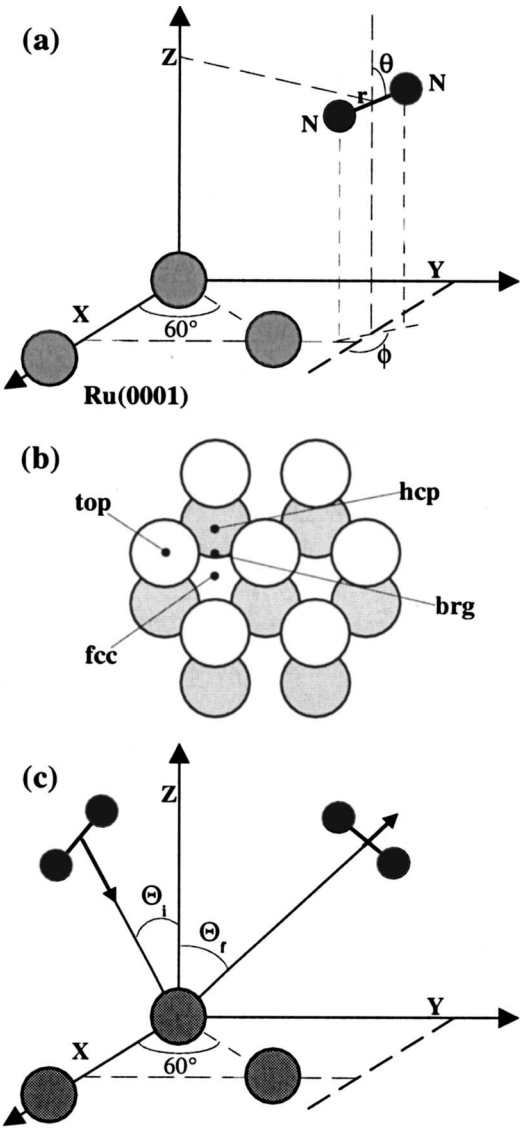

FIG. 1. (a) The coordinate system used to define the position and orientation of N_2 relative to the Ru surface. (b) High symmetry points of the Ru(0001) surface. The white (gray) spheres denote atoms in the first (second) layer. Atoms in the third (fourth) layer are directly below the atoms in the first (second) layer. (c) Coordinate system used to describe the direction of the velocity vector of the incident and scattered N_2.

tering and associative desorption.[20–22] This is not the case for the N_2/Ru(0001) system. Moreover, the analysis of the LAAD experiments presented in Ref. 11 suggests that $\frac{2}{3}$ of the energy used by the molecule to overcome the barrier is lost to the surface.

Much recent theoretical effort has been invested in understanding these unusual experimental findings. In Ref. 4 a two-dimensional (2D) nonadiabatic tunneling model was proposed, in which only two-degrees of freedom (DOFs) of the molecule, r (N–N distance) and Z (molecule-surface distance), were taken into account in the dynamics [see Fig. 1(a)]. In this model the potential energy surface (PES) includes a physisorption term (V_{phys}), describing the gas phase molecule attached to the surface; a chemisorption term (V_{chem}), describing the sum of the N-atom surface potentials; and a nonadiabatic coupling potential to account for the transition between V_{phys} and V_{chem}. This model reproduces quite accurately the experimental S_0, but introduces a number of parameters that need to be adjusted. It is not yet clear whether these parameters mostly reflect the true system dynamics or rather the restricted number of molecular DOFs treated. Two other low dimensional models were proposed in Ref. 11: (i) A 2+1D$(r,Z;q)$ adiabatic model, in which not only r and Z are included, but also the coupling to surface phonons via a single Einstein oscillator (q).[23] This low dimensional adiabatic model failed completely at reproducing the experimental value of S_0, overestimating it by two orders of magnitude. (ii) A 2+2D$(r,Z;q,\Gamma)$ nonadiabatic model in which an additional coupling to electron-hole (e-h) pair excitations (Γ) is included via electronic friction and fluctuating forces.[24] Although this model gave reaction probabilities in semiquantitative agreement with experiment, this agreement was only obtained by using a very strong nonadiabatic coupling, which was 12 times larger than that required for the description of vibrational damping of $O_2(v=1)$ adsorbed on Pt(111).[25] The question in this case is then whether such a strong nonadiabatic coupling is physically reasonable. A recent low dimensional theoretical study,[26] aiming to quantify the influence of nonadiabatic effects on the reactivity of N_2 +Ru(0001), suggests a smaller role of nonadiabatic effects, but the low dimensionality of the dynamical model does not allow one to reach a firm conclusion.

The low dimensional calculations were mainly focused on the influence of nonadiabatic effects and on how to include them in the dynamics. The influence of nonadiabatic effects on molecule-surface reactions has become a hot topic in the last few years, thanks to recent experiments showing direct evidence of nonadiabatic effects in molecule-surface scattering such e-h pair excitations accompanying chemisorption of atoms and molecules,[27] and ejection of electrons from low work function metal surfaces accompanying scattering of highly vibrationally excited molecules with high electron affinity.[28] These experiments might be viewed as questioning the validity of the Born-Oppenheimer (BO) approximation[29] for molecule-surface reactions. As discussed in Ref. 30, one reason that the BO approximation could seem suspect for the scattering of molecules from metal surfaces is that the metal surface electronic states exhibit a continuum energy distribution. Nevertheless this approximation has been used successfully in modeling molecule-surface reactions for a large number of systems[18,31,32] and in modeling heterogeneous catalysis.[33,34] On the other hand, recent theoretical work has shown that for some special systems, such as a high-spin molecule (O_2) (Ref. 35) and/or molecules of high electron affinity (O_2 and NO)[36] reacting on a metal surface with a low density of states at the Fermi level [Al(111)], the reaction can be better described using a nonadiabatic (diabatic with[36] or without coupling[35]) model.

In the case of N_2, we have a low-spin molecule of low electron affinity, so that, in principle, nonadiabatic effects are expected to be less important. Low dimensional results seem to contradict this expectation (see discussion above), giving rise to the following questions: Is N_2/Ru(0001) another special system for which the adiabatic approximation fails to account for experimental results on reaction, or are the molecular DOFs associated with rotation and translation parallel

to the surface perhaps more important for this system than for other systems?[37] In order to give appropriate answers to these questions we present here a six-dimensional (including the six DOFs of the molecule) adiabatic (neglecting e-h pair excitations) study of N_2 interacting with a Ru(0001) surface. Assuming the system to be reasonably well described by density functional theory (DFT) and the dynamics method employed (see below), the difference between the computational results and experiments should then allow for a verdict on the importance of nonadiabatic effects for this particular system.

The paper is organized as follows: In Sec. II we describe the methodology used, i.e., the electronic structure method used to compute the molecule-surface interaction energies, the interpolation of the potential, and the quasiclassical trajectory (QCT) method used in the dynamics calculations. In Sec. III we first present the main features of the six-dimensional (6D) PES obtained for N_2/Ru(0001), and then we discuss the dynamics results obtained for dissociative adsorption and scattering. A short account of some of the results obtained for dissociative adsorption has been published elsewhere.[38] Finally, we summarize the main conclusions in Sec. IV.

II. THEORY

To build the 6D PES for the N_2/Ru(0001) system we have used the modified Shepard (MS) interpolation method[39,40] adapted for molecule-surface reactions,[41] a new feature being that for the first time we use a direct interface to DFT. We have considered the six DOFs of the molecule: r, Z, the coordinates X and Y that represent the motion parallel to the surface, and the orientation of the molecule described by the polar (θ) and the azimuthal (ϕ) angles [see Fig. 1(a)]. We have made two main approximations: (i) We take the surface as frozen, i.e., we consider the surface atoms fixed in their equilibrium positions. Although N_2 is a heavy molecule and some energy exchange with the surface could be expected, this approximation is justified, to some extent, by the experimental results showing dissociation probabilities to be independent of surface temperature (T_s).[3,4] (ii) The BO approximation is applied, neglecting possible nonadiabatic effects (such as e-h pair excitations).

A. Electronic structure calculations

The electronic structure data points have been computed with DFT using the DACAPO code.[42] The generalized gradient approximation (GGA) is used in the description of the exchange-correlation energy of the electrons. In applying the GGA we have used the RPBE functional, which gives smaller overbinding and more accurate chemisorption energies than the PW91 functional,[43] and which has been shown to perform well in modeling ammonia production.[34] The ion cores were described using nonlocal ultrasoft pseudopotentials[44] (USPPs) (with core cutoff radii of $r_c^{\mathrm{N}}=0.6a_0$ and $r_c^{\mathrm{Ru}}=0.9a_0$) and a plane wave basis set was used for the electronic orbitals.

The adsorbate/substrate system is modeled using a three-layer slab and a 2×2 surface unit cell. The interlayer distance ($c/2$) was relaxed, and had a final value of 2.12 Å, slightly compressed with respect to the calculated bulk case (2.18 Å). A vacuum layer of 13.03 Å was placed between the slabs in the Z direction to avoid artifacts caused by the use of periodic boundary conditions in the direction perpendicular to the slab. To sample the Brillouin zone we have used a set of 18 Chadi-Cohen k points.[45] The cutoff energy for the plane wave basis was set at 350 eV. Using these parameters the molecule-surface interaction energies are converged to within 0.1 eV of the RPBE results for the given USSPs. We have found a minimum energy barrier of 2.27 eV in qualitative agreement with a previous calculation,[5] in which a value of about 2.4 eV was found for the molecule parallel to the surface and dissociating in the bridge to hollow geometry.

B. Interpolation method

In the MS interpolation method, the interpolated PES is given by a weighted series of Taylor expansions centered on DFT data points, sampled throughout the configuration space of the system. To get a physically more reasonable behavior when two atoms are close to each other, the inverse interatomic distances, $Q_i=1/R_i$ (R_i are the interatomic distance that defines the system), are used instead of the direct interatomic distances.[46] Thus, any configuration of the system is defined by the vector $\mathbf{Q}=[1/R_1,\ldots,1/R_{n(n-1)/2}]$, where n is the number of atoms needed to model the system. To model our system we use five atoms, two describing the N_2 approaching the Ru(0001) surface, and three atoms, which are kept fixed, to model the frozen surface.[41]

For each geometry $\mathbf{Q}$ a set of $3n$-6 algebraically independent linear combinations of the $n(n-1)/2$ interatomic distances, $\zeta(Q)$, can be defined in terms of the inverse distances as[47]

$$\zeta_m=\sum_{k=1}^{n(n-1)/2} U_{mk}Q_k \quad (m=1,\ldots,3n-6), \tag{1}$$

where U_{mk} is the transformation matrix from Cartesian coordinates to reciprocal bond lengths (see Ref. 47 for details). The potential energy at a configuration $\mathbf{Q}$, in the vicinity of a data point $\mathbf{Q}(i)$, can be expanded as a second-order Taylor expansion $T_i(\mathbf{Q})$, in these coordinates,

$$T_i(\mathbf{Q})=V[\mathbf{Q}(i)]+\sum_{k=1}^{3n-6}[\zeta_k-\zeta_k(i)]\left.\frac{\partial V}{\partial\zeta_k}\right|_{\mathbf{Q}=\mathbf{Q}(i)} +\frac{1}{2}\sum_{k=1}^{3n-6}\sum_{j=1}^{3n-6}[\zeta_k-\zeta_k(i)][\zeta_j-\zeta_j(i)]\left.\frac{\partial^2 V}{\partial\zeta_k\partial\zeta_j}\right|_{\mathbf{Q}=\mathbf{Q}(i)} +\cdots, \tag{2}$$

where $V[\mathbf{Q}(i)]$, the value of the potential at $\mathbf{Q}(i)$, and the gradients at this point are computed analytically by DACAPO. The second derivates are computed from the gradients using forward differencing.

The total potential energy at any configuration $\mathbf{Q}$ is then taken as

TABLE I. Translational energies and rovibrational initial states used in the growth process. In all cases $J_i=0$. Energies are in eV.

v_i	0 (E_{rv}=0.142)					1 (E_{rv}=0.427)				
E_i	2.32	2.82	3.12	4.12	4.87	5.61	2.57	2.97	3.62	4.37	5.12

$$V(\mathbf{Q}) = \sum_{g \in G} \sum_{i=1}^{N_{\text{data}}} w_{goi}(\mathbf{Q}) T_{goi}(\mathbf{Q}), \tag{3}$$

where the term $T_{goi}(\mathbf{Q})$ represents a second-order Taylor expansion and $w_{goi}(\mathbf{Q})$ a normalized weigh function (see Refs. 41 and 48 for more details). N_{data} is the number of DFT data in the interpolation, G is the symmetry group, and $g \circ i$ denotes the transformation of the ith data point by the group element g. To take into account the full symmetry of the system, a sum is taken over both the DFT data points and their symmetry equivalent points.

C. Implementation of the MS method in GROW

Unlike other interpolation schemes (see, for instance, Refs. 49 and 50), in the MS method the sampling of DFT data points is nonuniform, the density of data points being higher in the so-called dynamically important regions, which are found performing classical trajectory simulations. The idea behind the GROW method is that to calculate observables from a chemical reaction dynamics simulation, we only need to know the PES in the region of space through which the molecules pass during the dynamics.

In order to choose an appropriate data set the following iterative scheme[39,40] is used.

(1) We start with an initial version of the PES, which only includes a few points located along several reaction pathways. In our case, the initial PES contained 70 initial points chosen along four reaction pathways, i.e., 19 for the top, 19 for the bridge, and 19 for the hollow configuration, these three reaction pathways corresponding to the highest symmetry sites of the surface [see Fig. 1(b)] and 13 points along a minimum energy pathway. The minimum energy pathway was found by minimizing the N_2/Ru(0001) interaction energy with respect to θ, ϕ, X, Y, and Z, while keeping r fixed, for several values of r.

(2) Using this initial PES a few classical trajectories (typically ten) are run (see below). In order to assure the accurate representation of the PES for the whole energy range in which we are interested to carry out our study, we have grown the PES using simultaneously several translational energies (only normal incidence is considered in the growth process) and two rovibrational initial states (see Table I). Along each trajectory the molecular geometries explored by the simulation are periodically stored.

(3) From the stored geometries a new point is chosen (and added to the PES) according to one of the two criteria (see Refs. 39 and 48 for more details): (i) The "h-weight" criterion, which is based on the assumption that the best location for a new point would be the region most frequently visited by the trajectories. Thus, according to this criterion, the new point is added in the region of the PES most frequently visited, as long as there are not many data points already representing this region in the PES data set. (ii) The "variance" criterion, which is based on the assumption that the accuracy of the PES will be best improved if the new point is added in the region where the determination of the energy is suspected to be the most inaccurate.

(4) Once the PES is updated by adding the new chosen point, we restart the growth process from (2).

(5) After about 100 points are added, the accuracy of the PES is checked by computing an accurate value of the desired observable (in our case the reaction probability) from a more extensive classical trajectory simulation (10 000 trajectories). The growth process is stopped when the observable is considered to be converged, within a given tolerance. The analysis of the convergence of the reaction probability, for several incidence energies and two initial vibrational states, is shown in Fig. 2, where we have represented the reaction probability as a function of the number of data in the PES. To obtain an accurate PES for N_2/Ru(0001) we have

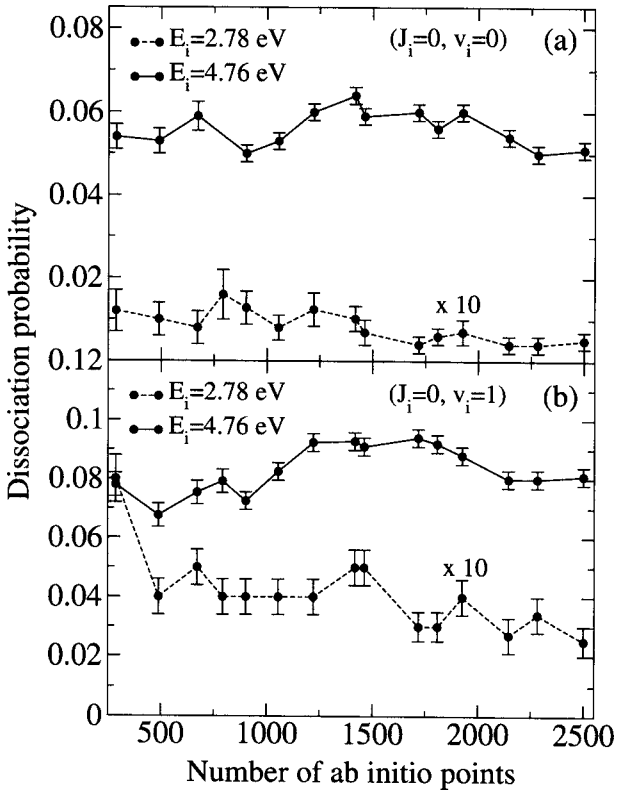

FIG. 2. The dissociation probability as a function of the number of DFT points added to the PES data set for two incidence energies, E_i=2.78 eV and E_i=4.76 eV. (a) v_i=0 and J_i=0; (b) v_i=1 and J_i=0.

computed 2500 DFT data points (70 initial points +2430 added points).

D. Quasiclassical dynamics

We have performed classical dynamics to find the dynamically important regions during the growth process and to compute reaction and scattering probabilities. In both cases, we have used the so-called QCT method,[51] in which the initial zero point energy (ZPE) of the molecule is included in the dynamics. Although these kinds of calculations are susceptible to the so-called ZPE violation problem (see Ref. 52), for an activated system this problem is expected to play a minor role at energies above the threshold to reaction. The QCT method generally gives accurate results for activated molecule-surface reactions.[53–56] Note that the vibrational softening (adiabatic transfer of energy from internal to translational motion) that takes place when the molecule approaches the surface is taken into account in the QCT method [its absence in the classical trajectory (CT) method leads to underestimated reaction probabilities[57]].

To compute the reaction and the scattering probabilities we have solved the classical equations of motion using the velocity-Verlet algorithm.[58] For each initial energy and initial rovibrational state, the probabilities are calculated as an average over the molecular initial conditions (internal coordinates and internal conjugated momenta). A Monte Carlo sampling method is used to simulate the molecular initial conditions for each set of initial parameters (E_i, v_i, and J_i). In order to obtain low statistical errors (typically between 10% and 3% depending on the translational energy E_i) we have computed 10 000 trajectories for each value of E_i and rovibrational state of N_2. We consider that dissociation has taken place whenever r reaches $5.0a_0$ with a positive radial velocity. The molecule is considered to be reflected whenever Z becomes equal to Z_i, Z_i being the initial distance between the molecule and the surface ($7.5a_0$), with the molecule's velocity vector pointing towards the vacuum.

III. RESULTS AND DISCUSSION

A. The N_2/Ru(0001) PES

The method used to build the PES allows us to locate easily the regions of the PES important for the dynamics, by merely looking at the distribution of points in configuration space. In Fig. 3 we show the computed DFT data points projected on the (Z,r) [Figs. 3(a) and 3(b)], (X,Y) [Figs. 3(c) and 3(d)], and $(\sin\theta,\phi)$ [Figs. 3(e) and 3(f)] hyperplanes. Looking at Figs. 3(a) and 3(b), we can see that most of the points are added in the entrance channel (valley of reactants), which reflects the low reactivity of N_2+Ru(0001). We can also see that for the highest energy (for both initial states $v_i=0$ and $v_i=1$) there are more points added around the transition state (located at $r=3.4a_0$ and $Z=2.53a_0$) than for the lowest energy, which is consistent with the fact that the reactivity is higher for higher translational energies. Figures 3(c) and 3(d) show that the added points are uniformly distributed over the (X,Y) and $(\sin\theta,\phi)$ planes. The $(\sin\theta,\phi)$ representations show slightly higher concentrations of points around $\sin\theta=\pm1$, which, with the way we have defined θ in the classical dynamics, corresponds to the orientation of the molecule most favorable for dissociation.

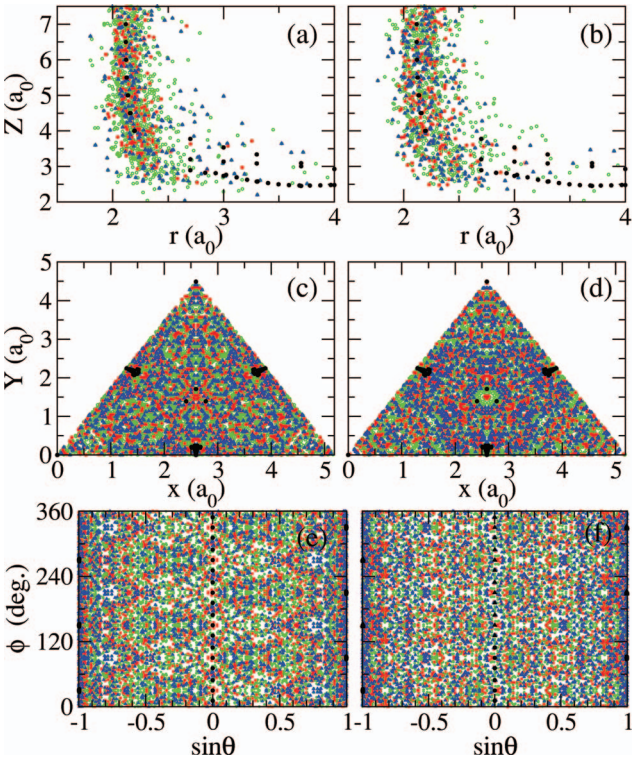

FIG. 3. (Color) The PES data set in (Z,r) representation [(a) and (b)], in (X,Y) representation [(c) and (d)], and in $(\sin\theta,\phi)$ representation [(e) and (f)]. The plots (a), (c), and (e) are obtained for $v_i=0$, and the plots (b), (d), and (f) for $v_i=1$. Black circles: initial DFT points; red squares: DFT points added for the lower energy growth; blue triangles: DFT points added for the higher energy growth; green circles: DFT points added for intermediate energy growth.

In Fig. 4 we show two 2D (r,Z) representations of the PES. We show two configurations for which the molecule approaches the surface with its N–N bond parallel to the surface ($\theta=90°$). In Fig. 4(a) the center of mass (c.m.) of the molecule is located over a top site [see Fig. 1(b)], while in Fig. 4(b) the c.m. is located halfway between a top site and a fcc site, with each N atom pointing toward a hcp site. We can see that both configurations present very high barriers towards reaction, which are located far in the exit channel, i.e., at large r. The second configuration is close to the lowest barrier ($V^*=2.27$ eV) geometry, which is located at $(X,Y,Z,r,\theta,\phi)=(1.4a_0,2.20a_0,2.53a_0,3.40a_0,86.23°,-29.33°)$. This PES does not only present high barriers but also very large anisotropy and corrugation. In Fig. 5 we show the energy profile near the minimum barrier geometry. From this figure we can see that both the anisotropy [Fig. 5(a)] and the corrugation [Fig. 5(b)] at the barrier are much larger for N_2/Ru(0001) than for the H_2/Cu system,[50] i.e., N_2/Ru(0001) presents a much narrower bottleneck towards reaction than H_2/Cu.

B. Dissociative adsorption

In this section we present reaction probabilities for normal incidence obtained using the QCT method. In order to

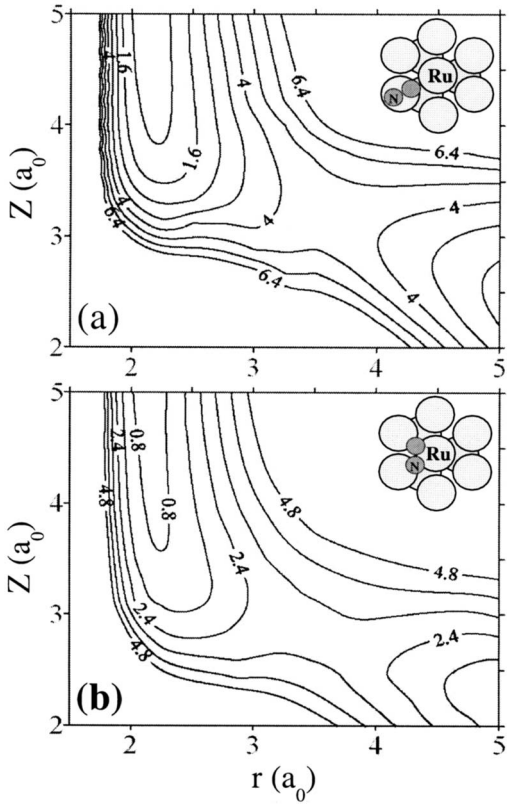

FIG. 4. 2D cuts through the PES for (a) the molecule approaching the top site with the N–N bond parallel to the surface (θ=90°) and (b) the molecule approaching a site halfway between the top and fcc sites, also with θ=90°. The potential is for the molecule oriented as indicated in the inset. The spacing between the contour levels is 0.8 eV.

compare our QCT results directly with the experimental ones, we have to include in our calculations the effect of the nozzle temperature (T_n), i.e., in principle we have to use the same rovibrational initial state distribution in our simulations as was presented in the experiments. To find the initial vibrational (v_i) state distribution corresponding to the different T_n, we assume that the vibrational temperature T_{vib} is approximately equal to T_n. The populations of the different initial vibrational states as a function of the simulated T_n are shown in Table II. To determine the initial rotational state distribution for a given T_n is not straightforward, because it depends not only on T_n but also on the experimental seeding and expansion conditions, i.e., it depends on the specific conditions under which each experiment was performed. However, as shown in Fig. 6 where we have plotted the reaction probabilities as a function of E_i for several J_i, the reaction probability does not depend significantly on the initial rotational state (J_i) for the J states with significant population at the rotational temperatures relevant to the molecular beams used in the experiments.[59] In fact, the reaction probabilities are the same to within the statistical accuracy of the calculations.

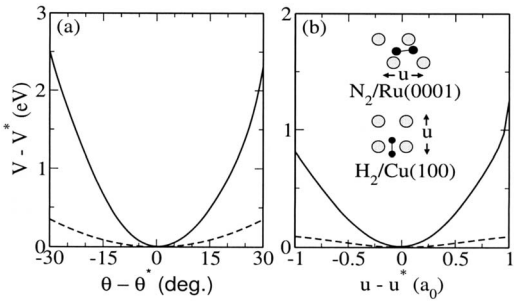

FIG. 5. The anisotropy and corrugation of the N_2/Ru(0001) (solid line) and H_2/Cu(100) (Ref. 50) (dashed line) potentials near the minimum barrier are illustrated by plotting the dependence of V-V^*, V being the potential and V^* the potential at the minimum barrier geometry, on θ (a) and u (b), keeping all other coordinates fixed to the barrier geometry Q^*. Here, u is the coordinate for motion along a straight line parallel to the surface, such that V varies the least.

TABLE II. Initial vibrational state distributions used in our QCT simulations.

T_n (K)	$P_{v=0}$ (%)	$P_{v=1}$ (%)	$P_{v=2}$ (%)
700	100	0	0
1850	83	14.5	2.5

In Fig. 7 we compare our 6D QCT reaction probabilities with some of the available experimental measurements.[4,9] The agreement between theory and experiment is remarkable. From the comparison between our 6D model and the 2+1D model (results of which are also included in Fig. 7) we see that the inclusion of the remaining four molecular DOFs (associated with rotation and translation parallel to the surface) decreases the reaction probability by two orders of magnitude. This illustrates the fundamental role played by these four DOFs. In fact, the inclusion of the rotation and parallel motions lowers the reaction probability much more for N_2/Ru(0001) than for the prototype system H_2/Cu(100).[18] This is due to the fact that, as has been shown in Sec. III A, both the corrugation and the anisotropy near the minimum barrier are much higher for N_2/Ru(0001) than for H_2/Cu(100). Thus the barrier is a much narrower bottleneck for N_2/Ru(0001) system, explaining the lower reactivity.

By looking more carefully at the comparison between 6D adiabatic theory and experiment for the higher E_i at which measurements are available (see inset in Fig. 7), we see that 6D QCT dynamics overestimates reaction probabilities by a factor of about 3 at the highest E_i for which experimental results are available (the nonadiabatic 2+2D model[11] overestimates S_0 by a factor of about 5). In the below analy-

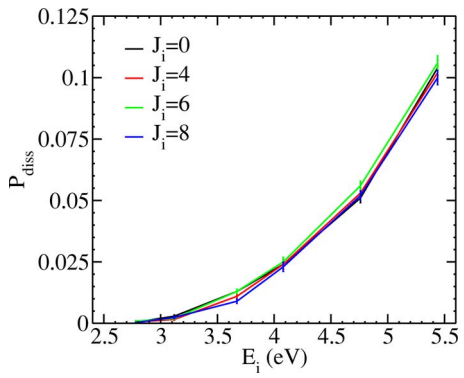

FIG. 6. (Color online) The reaction probabilities as a function of the translational energies for several initial rotational states J_i and v_i=0.

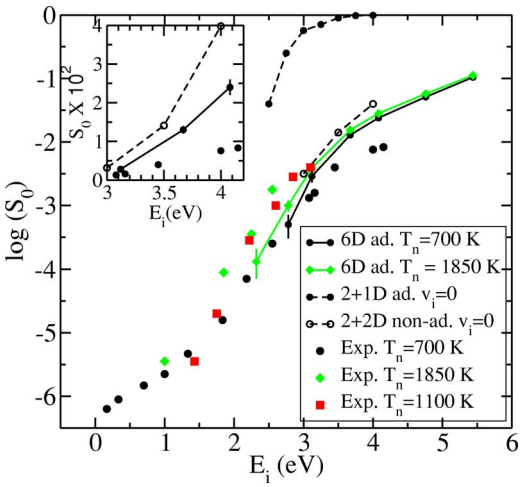

FIG. 7. (Color online) The log of the probability of N_2 dissociation on Ru(0001) is plotted vs normal translational energy E_i. The continuous line with full symbols represent 6D adiabatic calculations, the dashed line with full symbols represent 2+1D adiabatic calculations from Ref. 11, and the dashed line with open symbols 2+2D the nonadiabatic calculations from Ref. 11. Experimental measurements: full circles from Ref. 4, full green diamonds from Ref. 4, and full red squares from Ref. 9. The inset shows S_0 times 10^2 vs normal translational energy. Results are shown for different nozzle temperatures (T_n).

sis, we assume the experimental reaction probabilities[4,9] to be accurate, even though there could be considerable uncertainty in their absolute value, for instance, due to the procedure comparing the temperature programed desorption (TPD) of the small amount of N_2 adsorbed to that of a monolayer N_2.[59,60] Other sources of error are in the determination of the collision energy and of the flux.[60] These factors should, however, lead to an error of no more than a factor of 2 in the reaction probability ($\approx$0.01) measured at the highest E_i ($\approx$4 eV).[60]

In the theory, several factors can then be responsible for the remaining disagreement between experiment and 6D adiabatic theory: (i) approximations made in the implementation of the adiabatic frozen surface model, (ii) exclusion of phonons, and (iii) exclusion of e-h pair excitations. Concerning (i), although DFT is, in principle, an exact theory and has allowed the calculation of quite accurate dissociation probabilities for H_2-metal systems,[18,32] in practice its use requires some approximations. For instance, the exact form of the exchange-correlation functional is unknown, and the use of pseudopotentials to describe the ion cores is also a source of possible inaccuracies. These approximations lead to some uncertainties in the barrier heights of the system[61] and, therefore, also in the reaction probabilities. We have chosen to use the RPBE GGA functional[43] instead of the, at present, most used PW91 functional.[62] The RPBE functional has been selected because of the following: (a) The PW91 functional fails[34] to predict the barrier found experimentally (0.4 eV) for N_2+stepped Ru, which is, however, accurately described by the RPBE functional.[15] (b) The RPBE functional more accurately describes atomic and molecular chemisorptions on metal surfaces than the PBE functional, which gives values close to the PW91 functional.[43] (c) A recent systematic study[63] of the accuracy of several functionals for barrier heights in small gas phase systems shows a better agreement between RPBE results and results of more accurate hybrid functionals than between these hybrid functionals and the PW91 functional. The QCT method, as discussed above, has been shown to provide accurate results for activated dissociation of H_2 on metal surfaces,[53,55] H_2 presenting a much greater challenge to the classical approximation than N_2. Concerning (ii), although experimentally a minimal influence of T_s on reaction was found (for T_s between 500 and 850 K) within the classical regime ($E_i \geqslant V^*$),[3,4] this does not exclude the possibility that N_2 (which is rather heavy compared to H_2, for which the frozen surface approximation works quite well[31,64]) transfers energy to the metal surface phonons on impact. In fact, low dimensional calculations (including only r and Z) showed an increase in the classical reaction threshold of 0.5 eV upon inclusion of phonons. Although this result cannot be directly extrapolated to our 6D QCT calculations, it is likely that the inclusion of phonons will lower the reaction probability. Concerning (iii), in the case of e-h pair excitations the LAAD experiments[11] and experiments on vibrationally inelastic scattering,[13] as well as own our inelastic scattering study showing an overestimation of the energy transfer to molecular vibration (see Sec. III C), suggest that the remaining discrepancy between 6D adiabatic theory and experiment is, at least in part, due to nonadiabatic effects. Taking into account that the inclusion of phonons should also reduce the reaction probability, we can establish the factor of 3 discrepancy observed between 6D adiabatic theory and experiment at the highest E_i (inset in Fig. 7) as a reasonable upper bound to the effect that e-h pair excitations might have on the reactivity, at high incidence energies (about 4 eV).

The experimental and theoretical probabilities increase considerably with T_n (Fig. 7). To study the effectiveness of initial vibrational excitation at increasing reaction, we have computed the vibrational efficacy, which is a measure of the relative importance of molecular vibration and translation for promoting reaction, and is given by

$$\eta(S_0) = \frac{[\epsilon_{v=0}(S_0) - \epsilon_{v=1}(S_0)]}{E_{\mathrm{vib}}(v=1) - E_{\mathrm{vib}}(v=0)}, \tag{4}$$

where E_{vib} is the molecule's vibrational energy in the gas phase and $\epsilon(S_0)$ is the energy required to obtain a reaction probability S_0 when the molecules are initially in a vibrational state v. To evaluate η we have computed initial vibrational state resolved dissociation probabilities (Fig. 8). For an energy range of 3.3–5.5 eV and S_0 between 2.5×10^{-2} and 0.1, the average value we compute for $\eta(S_0)$ is about 1.6 [as the value of $\eta(S_0)$ depends slightly on the value of S_0, we have computed $\eta(S_0)$ for four different values of S_0 obtaining values between 1.4 and 1.8]. Thus, in our 6D adiabatic model vibrational excitation promotes reaction more efficiently than normal translational energy E_i. This result is in reasonable agreement with a previous estimated value of 1.3,[5] where reaction probabilities were obtained from detailed balance. It is also in qualitative agreement with an analysis of the previous experiments.[4] To calculate the value of η from the molecular-beam results, we suppose $S_0(T_n = 700\ \mathrm{K}) = S_0(v=0)$ and $S_0(T_n = 1850\ \mathrm{K}) = (1-c)S_0(v=0) + cS_0(v=1)$, c being the fraction of molecules in $v=1$ at 1850 K assuming that only $v=0$ and 1 are populated. Doing

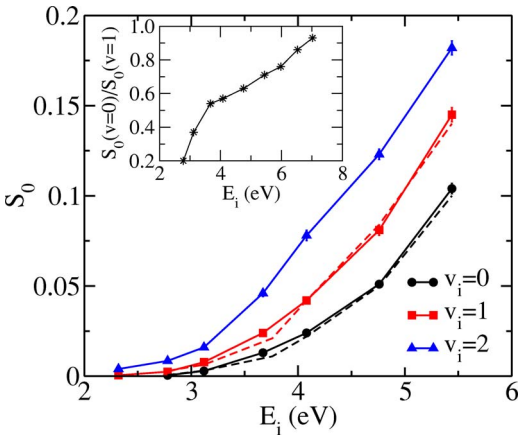

FIG. 8. (Color online) Computed dissociation probability vs incidence energy for several initial vibrational states v_i, and $J_i=0$. Continuous line: $^{14}N_2$. Dashed line: $^{15}N_2$. The inset shows the dissociation probability for $v_i=0$ divided by the dissociation probability for $v_i=1$ as a function of the incidence energy.

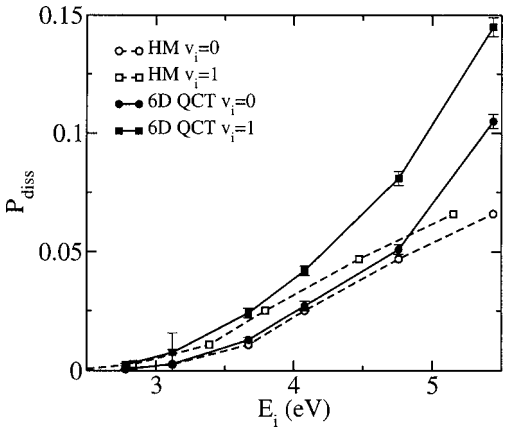

FIG. 9. The fraction of accessible 2D paths toward dissociation as a function of the translational energy. Solid lines and filled symbols: 6D QCT dissociative probabilities. Dashed lines and open symbols: hole model results.

this analysis we obtain $\eta \approx 3.8$. As we have neglected $v=2$ (also present for $T_n=1850$), we are overestimating the experimental value of η. We have evaluated this possible overestimation by doing a similar analysis of our $S_0(T_n)$, both including and excluding the $v=2$ contribution. Our analysis suggests that excluding the $v=2$ contribution to $S_0(T_n)$ leads to an overestimation of $\eta(S_0)$ by about 0.5. The result of this analysis of the efficacy is in contrast with a previous statement[9] that the effect should be less than for H_2/Cu ($\eta \approx 0.5$). However, this statement was not backed up by an analysis in terms of the vibrational efficacy. Although quantitatively there are discrepancies between our adiabatic results and previous experiments,[4] both show that excitation of the N_2 vibration promotes reaction much more efficiently than increasing the N_2 translational energy normal to the surface. A similar finding was mentioned in Ref. 15.

This high vibrational efficacy contrasts with the relatively low η found in other N_2/metal systems.[65,66] However, a similar high vibrational enhancement has been observed previously, for instance, for $CH_4/Ni(111)$.[67] It is worth noticing that in the case of $N_2/Ru(0001)$ the sticking curves for different v_i apparently saturate at about the same amplitude for $v=0$ and $v=1$ (see inset in Fig. 8); therefore, we can consider that all the v_i dependence is contained in η (see Ref. 68 for more details). Now the question is how the vibrational energy can be more efficient than E_i at promoting reaction. In principle, a vibrationally excited molecule has a maximum extra energy to overcome the barrier, $E_v=n\hbar\omega_0$ (n being the vibrational state), which means that, in principle, the vibrational excitation cannot reduce the E_i required to overcome the barrier by more than E_v. One possible explanation to this phenomenon was proposed in Ref. 67: a vibrationally excited molecule surmounting a late barrier can in some cases access phase space regions where the transition state is lower than those accessed by molecules in the vibrational ground state (see Fig. 3 of Ref. 67), which means that the reaction barrier seen by molecules in $v_i=1$ is smaller (by ΔE) than for molecules in $v_i=0$. Thus, the translation energy needed by a molecule in $v_i=1$ to overcome the barrier is reduced by $E_v+\Delta E$, which can explain how η can be bigger than 1.

In Fig. 8 we show the initial vibrational state resolved reaction probabilities for the heavier isotope $^{15}N_2$. Taking into account the statistical errors intrinsic to the calculation, no isotope effect is observed. This result is in perfect agreement with the experimental findings,[6] according to which isotope effects are only observed for incidence energies below the minimum reaction barrier (the quantum regime).

We now address the following fundamental question: Why is the reactivity so small in the $N_2/Ru(0001)$ system? As we have shown in Sec. III A, the system shows a very high anisotropy and corrugation around the minimum reaction barrier (see Fig. 5), which means that the potential seen by a molecule approaching the surface depends strongly on its position and orientation over the surface. Of course, in a 6D scenario all values of (X,Y,θ,ϕ) that are compatible with the given energy are allowed, which means, from a statistical point of view, that the number of molecules approaching the surface with a geometry favorable to dissociation is very small (smaller than in the case of H_2/Cu). On the other hand, if steering in the rotational and the translational motion parallel to the surface would be efficient enough to drive the molecule to the minimum energy reaction path, thereby avoiding the highest barriers when it approaches the surface, a strong corrugation and anisotropy would not be an impediment to reaction.

To study the efficiency of the dynamics to drive the molecule to the minimum energy reaction path, we have compared our 6D QCT results with that obtained using the hole model (HM).[69] In the absence of complex dynamical behavior, this static model allows a good guess of the dissociation probability for a fixed E_i, merely by looking at the fraction of molecular configurations leading to dissociation. From Fig. 9, there is a good agreement between the HM and QCT results for molecules in the vibrational ground state, for $E_i < 5$ eV, whereas for molecules with $v_i=1$ the agreement is only good for $E_i < 4$ eV. These results can be taken as an indication of the inefficiency of the rotational and parallel translational motions to drive the molecule to the minimum

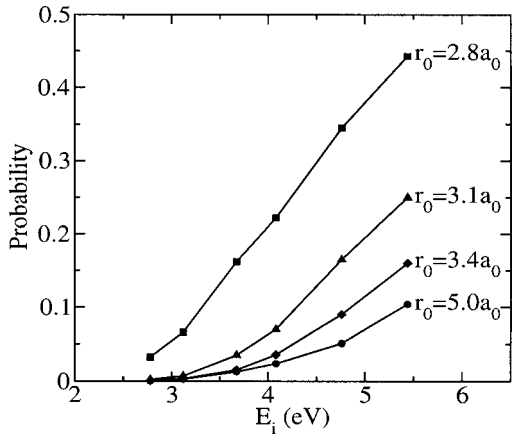

FIG. 10. The probability of the molecule to reach an interatomic distance r_0, with $r_0=3.4a_0$ being the minimum reaction barrier and $r_0=5a_0$ is the dissociation condition.

energy reaction path. When E_i increases, the rotations become more efficient at steering the molecule towards the reaction path, because the high force zones of the PES start to play a predominant role.[70] This explains the difference between the HM probability and the 6D QCT results at high energies. In summary, the reaction probability is small at energies significantly above the minimum barrier height not only because of the presence of a narrow minimum reaction barrier but also because of the nature of the dynamics, which does not allow the molecule to get oriented or positioned in such a way as to be able to pass the barrier. In fact, most of the molecules do not even approach the barrier, they are scattered back to the vacuum far from the minimum reaction barrier, as we can see in Fig. 10, where we have plotted the probability of a molecule to reach an interatomic distance r_0 (see Sec. III A).

C. Scattering

As we have shown in Sec. III B reaction is the minority process for N_2 interacting with Ru(0001). Now we are going to focus on the majority process, scattering. Some extra information about the system can be extracted by looking at the molecules scattered back to the vacuum after the interaction with the surface. Experimentally it is not possible to study scattering under normal incidence conditions; therefore, most of the results we present in this section are for non-normal incidence. We defined the incidence angle Θ_i as the angle between the incident velocity vector and the surface normal [see Fig. 1(c)].

In Fig. 11(a) we present the angular distribution of the scattered molecules, for an incidence angle $\Theta_i=40°$. We can see that the maximum of the distribution increases and its fullwidth at half maximum (FWHM) decreases with incidence energy until $E_i=0.41$ eV, and then the maximum decreases and the FWHM increases with E_i. A similar behavior has been found experimentally.[12] In Fig. 11(b) we have plotted the FWHM as a function of the incidence energy for $\Theta_i=40°$ and 50°. We see that for 50° the increase of the FWHM with E_i is less pronounced and starts at a higher E_i. It has been argued[12] that this behavior is related to the existence of two scattering regimes: thermal scattering should dominate at low incident energies, whereas structural scattering should dominate at high energies. The argument is that, in structural scattering, at higher normal energies ($E_\perp$) the molecule sees a more corrugated surface (higher penetration[71]), leading to a bigger momentum exchange and a broader distribution, consistent with the experimental and theoretical results. For the same incidence angle, $E_\perp$ increases with E_i, leading to an increase of FWHM with E_i, and for the same incidence energy, $E_\perp$ decreases with increasing Θ_i, leading to a smaller FWHM at $\Theta_i=50°$. For low incidence energies, the argument of thermal scattering cannot be applied to our theoretical results (which nevertheless show a decrease of the FWHM with E_i like the experimental results), because we consider the surface atoms fixed in their equilibrium position (see Sec. II). The behavior of the FWHM at low E_i can, however, also be understood without invoking the effect of the phonons. For low E_i the molecules are reflected far from the surface, and for the energy range of 0.05–0.41 eV the corrugation seen by the molecules is more or less the same, which implies that the momentum exchange is similar for the smaller energies (see inset in Fig. 12). This implies that the relative momentum exchange, defined as $|\Delta K|/K_i$, should decrease with increasing E_i. The relative momentum exchange is directly related to the width of the angular distribution: the bigger the relative momentum exchange, the broader the angular distribution is expected to be and vice versa. From Fig. 12 we observe that the relative

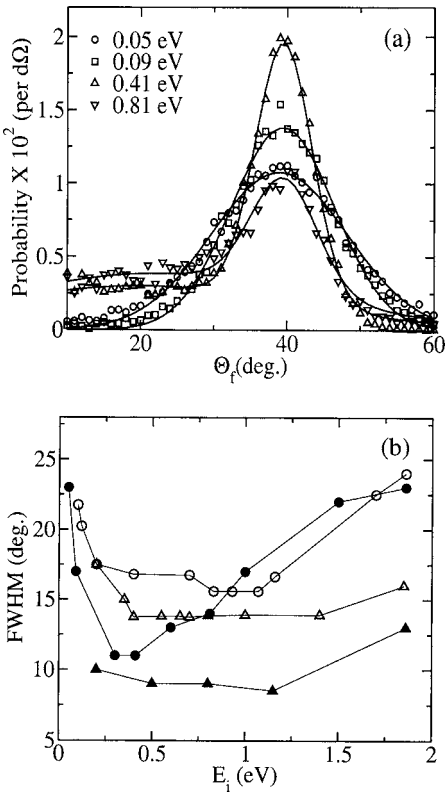

FIG. 11. (a) The reflection probabilities per unit solid angle as a function of Θ_f, for $\Theta_i=40°$ and several E_i. The continuous lines through the data points are to guide the eye only. (b) The width of the angular distribution as a function of E_i. Open symbols: experimental data (Ref. 12); filled symbols: our theoretical results. Circles: $\Theta_i=40°$; triangles: $\Theta_i=50°$.

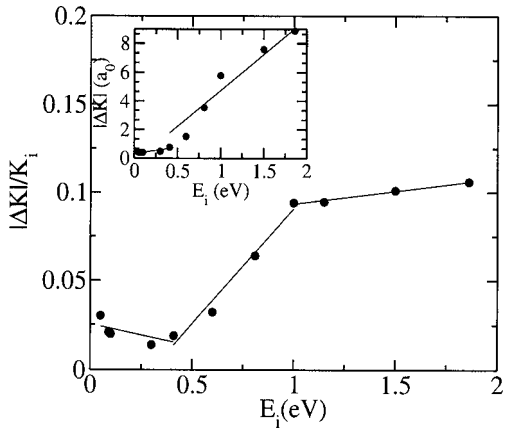

FIG. 12. The relative momentum exchange as a function of the incidence energy for $\Theta_i=40°$. The continuous lines through the data points are to guide the eye only.

momentum change indeed decreases with E_i until $E_i \approx 0.41$ eV and from this point on increases with E_i. Comparing Figs. 12 and 11(b) we see that the minimum of the FWHM of the angular distribution agrees with the minimum of the relative momentum exchange curve.

Other interesting features that we can extract from the scattered molecules, which contain information about the interaction between the molecule and the surface, are energy transfer to the molecule's internal motion and to the parallel translational motion. The average energy transferred to translation parallel to the surface ($\langle \Delta E_x \rangle$) as a function of E_i is shown in Fig. 13(a), along with the available experimental results.[13] Both theory and experiment show a small excitation of the translational energy parallel to the surface, which increases which increasing E_i (and $E_\perp$, for high E_i). As explained above, when $E_\perp$ increases the molecules get closer to the surface and experience more corrugation, which favors the excitation of the parallel motion via momentum exchange. In the theory, for the higher energies we observe a clear difference between the results for the initial conditions $\Theta_i=19°$ and $\Theta_i=40°$: $\langle \Delta E_x \rangle$ is twice as high as for the first condition. Two factors can explain this difference: (i) Penetration (and therefore corrugation) is expected to be increased when Θ_i decreases.[71] (ii) For $\Theta_i=19°$ there is a much bigger difference between the normal and the parallel energy, which favors the transfer of energy from normal to parallel motion. From the experimental data it is not possible to establish any kind of dependence of ΔE_x on Θ_i, due to the magnitude of the errors and the small number of points for $\Theta_i=40°$.

Rotational excitation is overestimated in our theoretical calculations in comparison with the experimental findings,[13] as can be observed in Fig. 13(b), where we have plotted the average of the energy transferred to rotation ($\langle \Delta E_{\text{rot}} \rangle$) as a function of the incidence energy, for $J_i=0$. The disagreement between theory and experiment increases with E_i, and the theoretical value $\langle \Delta E_{\text{rot}} \rangle$ becomes twice the experimental one at $E_i \approx 2.8$ eV. The disagreement between theory and experiment is even worse for vibrational excitation [see Fig. 13(c)]. In this case, the theoretical average of the energy transferred to vibration $\langle \Delta E_{\text{vib}} \rangle$ is around seven times bigger than the

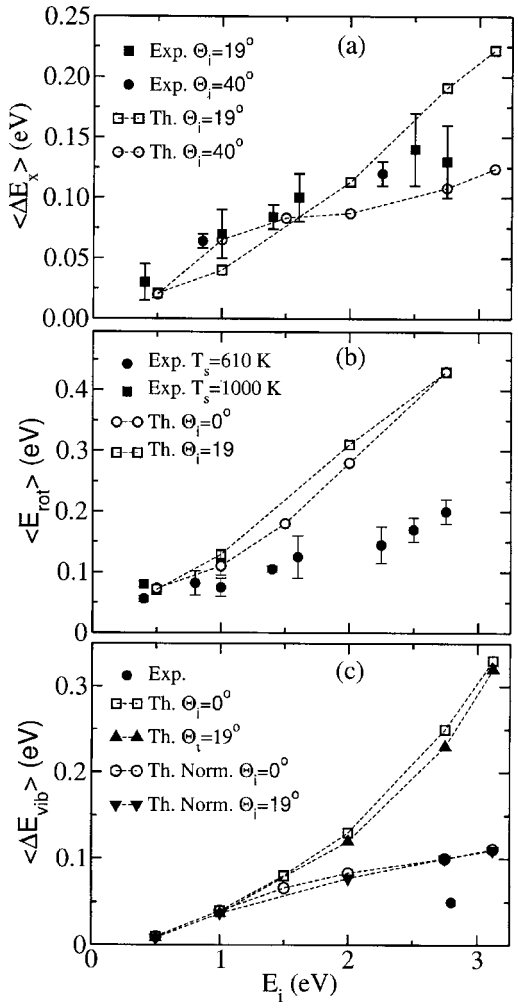

FIG. 13. (a) The conversion of incidence energy E_i into translational energy parallel to the surface, ΔE_x, as a function of the incidence energy. The filled symbols are from experiment (Ref. 13). (b) The average of the energy transfered to rotation $\langle \Delta E_{\text{rot}} \rangle$ as a function of the translational energy. (c) The average of the energy transfered to vibration $\langle \Delta E_{\text{vib}} \rangle$ as a function of the translational energy. "Norm" means that we suppose $P_{\text{ref}}(v_f=0)+P_{\text{ref}}(v_f=1)=1$.

experimental one at $E_i=2.8$ eV (the only available experimental data[13]). Experimentally no measurable vibrational excitation was observed; the value given in Fig. 13(c) is merely an upper bound determined to $v=1$ excitation. It is not clear whether an attempt was made to measure vibrational excitation to $v>1$. The lack of vibrational excitation in this experiment was attributed in part to the spectral overlap associated with transitions of $v=0$, $J \geqslant 49$ and the low J transitions of $v=1$. Taking into account that experiments did not consider transitions to $v>1$ we have recalculated the $\langle \Delta E_{\text{vib}} \rangle$ as it would be measured in experiments only considering scattering to $v=0$ and 1, i.e., we suppose that $P_{\text{ref}}(v_f=0)+P_{\text{ref}}(v_f=1)=1$, where $P_{\text{ref}}(v_f)$ is the probability that a reflected molecule is scattered to the final state v_f. Figure 13(c) shows that when making this supposition our theoretical $\langle \Delta E_{\text{vib}} \rangle$ is lowered to a value that is only twice the experimental value (a difference similar to that found for rotational excitation).

Classical dynamics is not the best method to study energy transfer to molecule's internal motions, because the selection rules limiting this transfer are not taken into account.

Quantum mechanically only transitions between internal energy states with $\Delta v=n$, n being 0,1,2,…, and $\Delta J=2n$ (because of the nuclear spin symmetry) are allowed for N_2, whereas classically the internal energy transfer presents a continuous distribution. Nevertheless, it has been shown previously that classical dynamics can account for some typical quantum features such as rotational excitation[72] or even diffraction.[73] The main problem classical dynamics face in this kind of studies is how to use "binning," i.e., how to transform a continuous distribution into a discrete representation. In the case of rotational excitation we have checked our results using two different binning methods: (i) "Homogeneous binning," in which we assign J to reflected molecules by evaluating the closest integer that satisfies $J_{cl}=[-1+(1+4L^2/\hbar^2)^{1/2}]/2$ and $\Delta J=2n$, where L is the classical angular momentum, and we consider all trajectories to have the same weight in the final discrete distribution. (ii) "Nonhomogeneous binning,"[74] where each trajectory is weighted by a Gaussian-type coefficient such that the closer the J_{cl} values to integer values satisfying $\Delta J=2n$, the larger the coefficient. Both methods (i) and (ii) allow one to choose $\Delta J=n$ or $2n$ $(n=0,1,2,\ldots)$. No significant differences in the results have been found using these two methods with the rule $\Delta J=2n$, which seems reasonable due to the small energy spacings between the rotational levels of N_2. This suggests that the disagreement between theory and experiment for the rotational energy transfer cannot be attributed to deficiencies of the QCT method.

The agreement between the scattering experiments and our 6D adiabatic calculations can also be affected by the use of the frozen surface approximation. Although the phonons seem to play a minor role for dissociative chemisorption, they could be important for rotational excitation, because the energy spacings between the rotational levels are small. As we do not include the phonons in our calculation we can only speculate about their effect using the previous experimental and theoretical results. Low dimensional calculations suggest that the inclusion of phonons in the dynamics increases the reaction threshold. This means that the molecule looses energy to the surface, thus less energy is available for rotational excitation and therefore the inclusion of phonons could lead to less rotational and vibrational excitations. Of course, once the phonons are taken into account the rotational excitation is expected to increase with T_s, the larger T_s the smaller the transfer of energy from the molecule to the surface is expected, and then more energy is available for rotational excitation. The increase of rotational excitation with T_s has been observed experimentally.[13]

It has been suggested[13] that the absence of observable vibrational excitation in the experiment could be due to nonadiabatic coupling to e-h pair excitations. This conclusion is partly based on the previous observation of significant vibrational excitation and deexcitation for another "exit" channel system, $H_2(D_2)/Cu(111)$,[20] for which e-h pair excitations are expected to be unimportant, and also on the comparison between adiabatic and nonadiabatic low dimensional calculations (see above). But, as we have shown in Sec. III, $N_2/Ru(0001)$ presents large differences with the other prototype exit channel system, $H_2+Cu(111)$, and low dimensional calculations cannot be used to describe the dynamics of this system properly. On the other hand, our adiabatic 6D calculations do show more vibrational excitation than the experiments, and we cannot rule out that this is due to the absence of e-h pair excitations in our model. To obtain more insight in the role of phonons and e-h pair excitations, 6+2D calculations should be done in a fashion similar to that used in the 2+2D model of Diekhöner *et al.*,[11] using an appropriate coupling strength parameter describing the nonadiabatic coupling.[26]

IV. SUMMARY AND CONCLUSIONS

In this paper we have presented a six-dimensional (6D) quasiclassical dynamics study, within the adiabatic approximation, of N_2 reacting with and scattering from a Ru(0001) surface. The 6D potential energy surface (PES) has been constructed applying a modified Shepard method to a nonuniform set of electronic structure data, which are chosen using quasiclassical dynamics. The electronic structure data were obtained with density functional theory, using the RPBE generalized gradient approximation in a supercell approach.

The dissociative adsorption probabilities computed using 6D quasiclassical dynamics show good agreement with previous experimental results, with a very low reaction probability for incidence energies significantly above the minimum reaction barrier. A comparison with previous calculations using a 2+1D adiabatic model including phonons shows that the inclusion, in both a static description using the hole model (HM) and in the dynamics, of the four DOFs of the molecule associated with the rotation and translation parallel to the surface lowers the reaction probability by two orders of magnitude. Furthermore, the good agreement between the experimental and the HM probability shows that the low reactivity of the system can already be understood by looking only at the static properties of the PES. Our results show clearly that the previous experimental findings can be explained largely within an adiabatic framework, without invoking large nonadiabatic effects, if the six DOFs of the molecule are included in an accurate description of the PES. The low reactivity of the system reflects the high anisotropy and corrugation of the potential, making the barrier a very narrow bottleneck to reaction.

Theoretical angular scattering distributions show the same behavior as observed experimentally. In agreement with experiment, two scattering regimes can be distinguished: one operating at low energy and one at high energies. At high energies the decrease of the maximum of the distribution and the increase of its width with energy are due to the increase of the corrugation seen by the molecules (structure scattering). For low energies, the calculations suggest that the decrease of the width of the distribution with energy is not (entirely) due to the interaction with the surface phonons, because it is also observed in our static surface calculations. Instead, it reflects a decrease of the relative momentum exchange as the incidence energy is increased in a regime where structural scattering does not yet occur.

Finally, whereas our theoretical results show a small ex-

citation of the translation parallel to the surface increasing with E_i, in good agreement with the experiment, rotational and vibrational excitations are overestimated by our theoretical calculations. Additional work is needed in which motion in all six N_2 DOFs is considered alongside dissipation to phonons and electron-hole (e-h) pair excitations to explain these discrepancies.

Although our study by itself cannot be used to determine in an accurate way the influence of the e-h pair excitations on the interaction between N_2 and Ru(0001), it allows us, at least, to determine (assuming the experiments to be accurate and considering the factors that affect the accuracy in the theory) an upper bound to the influence that nonadiabatic effects have on the reactivity of this system. This influence is much smaller than previously suggested by low dimensional calculations: Our calculations suggest that at the highest incidence energies considered, e-h pair excitations diminish the reactivity by no more than a factor of 3, rather than by two orders of magnitude as suggested by the previous low dimensional calculations. On the other hand, it is essential to take into account the multidimensional effects (rotation and translation parallel to the surface) in the dynamics for an appropriate description of the system. This reduces the reactivity by two orders of magnitude. The minor role played by nonadiabatic effects in dissociative chemisorption of N_2 on Ru(0001) can be understood from recent theoretical work, which strongly suggests that a breakdown of the Born-Oppenheimer approximation should be expected for (i) molecules with high electron spin interacting with a metal surface with a low density of states at the Fermi level, due to spin quenching before the systems interact;[35] and (ii) molecules with intermediate electronegativities, for which the time scale for the electron transfer process and the nuclear motion are comparable.[36] N_2 has zero electronic spin, so that nonadiabatic spin quenching is not possible, and it also has a low electronegativity so that no nonadiabatic effects accompanying electron transfer from the surface to the molecule expected.

ACKNOWLEDGMENTS

The authors would like to thank Professor A. Salin for useful discussions. This work was financially supported by the European Commission through the research training network "Predicting Catalysis" under Contract No. HPRN-CT-2002-00170.

[1] T. Matsushima, Surf. Sci. **197**, L287 (1988).
[2] H. Shi, K. Jacobi, and G. Ertl, J. Chem. Phys. **99**, 9248 (1993).
[3] H. Dietrich, P. Geng, K. Javobi, and G. Ertl, J. Chem. Phys. **104**, 375 (1996).
[4] L. Romm, G. Katz, R. Kosloff, and M. Asscher, J. Phys. Chem. B **101**, 2213 (1997).
[5] M. J. Murphy, J. F. Skelly, A. Hodgson, and B. Hammer, J. Chem. Phys. **110**, 6954 (1999).
[6] L. Romm, O. Citri, R. Kosloff, and M. Asscher, J. Chem. Phys. **112**, 8221 (2000).
[7] L. Diekhöner, H. Mortensen, A. Baurichter, A. C. Luntz, and B. Hammer, Phys. Rev. Lett. **84**, 4906 (2000).
[8] L. Diekhöner, H. Mortensen, A. Baurichter, and A. C. Luntz, J. Chem. Phys. **115**, 3356 (2001).
[9] L. Diekhöner, H. Mortensen, A. Baurichter, E. Jesen, V. V. Petrunin, and A. C. Luntz, J. Chem. Phys. **115**, 9028 (2001).
[10] R. C. Egeberg, J. H. Larsen, and I. Chorkendorff, Phys. Chem. Chem. Phys. **3**, 2007 (2001).
[11] L. Diekhöner, L. Hornekaer, H. Mortensen, E. Jensen, A. Baurichter, V. V. Petrunin, and A. C. Luntz, J. Chem. Phys. **117**, 5018 (2002).
[12] D. C. Papageorgopoulos, B. Berenbak, M. Verwoest, B. Riedmuller, S. Stolte, and A. W. Kleyn, Chem. Phys. Lett. **305**, 401 (1999).
[13] H. Mortensen, E. Jensen, L. Diekhöner, A. Baurichter, A. C. Luntz, and V. Petrunin, J. Chem. Phys. **118**, 11200 (2003).
[14] J. J. Mortensen, Y. Morikawa, B. Hammer, and J. K. Nørskov, J. Catal. **169**, 85 (1997).
[15] S. Dahl, A. Logadottir, R. C. Egeberg, J. H. Larsen, I. Chorkendorff, E. Tornqvist, and J. K. Nørskov, Phys. Rev. Lett. **83**, 1814 (1999).
[16] S. Dahl, E. Tornqvist, and I. Chorkendorff, J. Catal. **192**, 381 (2000).
[17] R. v. Harrevelt, K. Honkala, J. K. Nørskov, and U. Manthe, J. Chem. Phys. **122**, 234702 (2005).
[18] G. J. Kroes, A. Gross, E. J. Baerends, M. Scheffler, and D. A. McCormack, Acc. Chem. Res. **35**, 193 (2002).
[19] M. F. Somers, D. A. McCormack, G. J. K. R. A. Olsen, E. J. Baerends, and R. C. Mowrey, J. Chem. Phys. **117**, 6673 (2002).
[20] C. T. Rettner, D. J. Auerbach, and H. A. Michelsen, Phys. Rev. Lett. **68**, 2547 (1992).
[21] C. T. Rettner, H. A. Michelsen, and D. J. Auerbach, J. Chem. Phys. **102**, 4625 (1995).
[22] G. J. Kroes, G. Wiesenekker, E. J. Baerends, and R. G. Mowrey, Phys. Rev. B **53**, 10397 (1996).
[23] M. Hand and J. Harris, J. Chem. Phys. **92**, 7610 (1990).
[24] M. Head-Gordon and J. C. Tully, J. Chem. Phys. **103**, 10137 (1995).
[25] B. N. J. Persson, Chem. Phys. Lett. **139**, 457 (1987).
[26] A. C. Luntz and M. Persson, J. Chem. Phys. **123**, 074704 (2005).
[27] B. Gergen, H. Nienhaus, W. H. Weinberg, and E. W. McFarland, Science **294**, 2521 (2001).
[28] J. D. White, J. Chen, D. Matsiev, D. J. Auerbach, and A. M. Wodtke, Nature (London) **433**, 503 (2005).
[29] M. Born and E. Oppenheimer, Ann. Phys. (Leipzig) **84**, 457 (1927).
[30] A. M. Wodtke, J. Tully, and D. J. Auerbach, Int. Rev. Phys. Chem. **23**, 513 (2004).
[31] G. R. Darling and S. Holloway, Rep. Prog. Phys. **58**, 1595 (1995).
[32] P. Nieto, E. Pijper, D. Barrero, G. Laurent, R. A. Olsen, E. J. Baerends, G. J. Kroes, and D. Farías, Science **312**, 86 (2006).
[33] K. Reuter, D. Frenkel, and M. Scheffler, Phys. Rev. Lett. **93**, 116105 (2004).
[34] K. Honkala, A. Hellman, I. N. Remediakis, A. Lagadottir, A. Carlsson, S. Dahl, C. H. Christensen, and J. K. Nørskov, Science **307**, 555 (2005).
[35] J. Behler, B. Delley, S. Lorenz, K. Reuter, and M. Scheffler, Phys. Rev. Lett. **94**, 036104 (2005).
[36] A. Hellman, B. Razaznejad, and B. I. Lundqvist, Phys. Rev. B **71**, 205424 (2005).
[37] G. J. Kroes, E. J. Baerends, and R. G. Mowrey, Phys. Rev. Lett. **78**, 3583 (1997).
[38] C. Díaz, J. K. Vincent, G. P. Krishnamohan, R. A. Olsen, G. J. Kroes, K. Honkala, and J. K. Nørskov, Phys. Rev. Lett. **96**, 096102 (2006).
[39] J. Ischtwan and M. A. Collins, J. Chem. Phys. **100**, 8080 (1994).
[40] R. P. A. Bettens and M. A. Collins, J. Chem. Phys. **111**, 816 (1999).
[41] C. Crespos, M. A. Collins, E. Pijper, and G. J. Kroes, J. Chem. Phys. **120**, 2392 (2004).
[42] DACAPO, http://dcwww.camp.dtu.dk/campos/Dacapo/
[43] B. Hammer, L. B. Hansen, and J. K. Nørskov, Phys. Rev. B **59**, 7413 (1999).
[44] D. Vanderbilt, Phys. Rev. B **41**, 7892 (1990).
[45] D. J. Chadi and M. L. Cohen, Phys. Rev. B **8**, 8747 (1973).
[46] R. G. Parr and R. J. White, J. Chem. Phys. **49**, 1059 (1968).
[47] K. C. Thompson, M. J. T. Jordan, and M. A. Collins, J. Chem. Phys. **108**, 8302 (1998).
[48] M. A. Collins, Theor. Chem. Acc. **108**, 313 (2002).
[49] H. F. Busnengo, A. Salin, and W. Dong, J. Chem. Phys. **112**, 7641 (2000).
[50] R. A. Olsen, H. F. Busnengo, A. Salin, M. F. Somers, G. J. Kroes, and E. J. Baerends, J. Chem. Phys. **116**, 3841 (2002).
[51] M. Karplus, R. N. Porter, and R. D. Sharma, J. Chem. Phys. **43**, 3259 (1965).
[52] Y. Guo, D. L. Thompson, and T. D. Sewell, J. Chem. Phys. **104**, 576 (1996).
[53] D. A. McCormack and G. J. Kroes, Phys. Chem. Chem. Phys. **1**, 1359 (1999).

[54] D. A. McCormack, G. J. Kroes, R. A. Olsen, I. A. Groeneveld, J. N. P. van Stralen, E. J. Baerends, and R. C. Mowrey, Faraday Discuss. **117**, 109 (2000).
[55] E. Pijper, M. F. Somers, G. J. Kroes, R. A. Olsen, E. J. Baerends, H. F. Busnengo, A. Salin, and D. Lemoine, Chem. Phys. Lett. **347**, 277 (2001).
[56] P. Riviere, H. F. Busnengo, and F. Martín, J. Chem. Phys. **123**, 074705 (2005).
[57] H. F. Busnengo, C. Crespos, W. Dong, J. C. Rayez, and A. Salin, J. Chem. Phys. **116**, 9005 (2002).
[58] W. C. Swope, H. C. Andersen, P. H. Berens, and K. R. Wilson, J. Chem. Phys. **76**, 637 (1982).
[59] A. C. Luntz (private communication).
[60] M. Asscher (private communication).
[61] J. K. Vincent, R. A. Olsen, and G. J. Kroes, J. Chem. Phys. **122**, 122 (2005).
[62] J. P. Perdew, J. A. Chevary, S. H. Vosko, K. A. Jackson, M. R. Pederson, D. J. Singh, and C. Fiolhais, Phys. Rev. B **46**, 6671 (1992).
[63] S. Andersson and M. Grüning, J. Phys. Chem. A **108**, 7621 (2004).
[64] G. J. Kroes, Prog. Surf. Sci. **60**, 1 (1999).
[65] C. T. Rettner and H. Stein, J. Chem. Phys. **87**, 770 (1987).
[66] G. Haase, M. Asscher, and R. J. Kosloff, J. Chem. Phys. **90**, 3346 (1989).
[67] R. R. Smith, D. R. Killelea, D. F. DelSesto, and A. L. Utz, Science **304**, 992 (2004).
[68] A. C. Luntz, J. Chem. Phys. **113**, 6901 (2000).
[69] M. Karikorpi, S. Holloway, N. Henriksen, and J. K. Nørskov, Surf. Sci. **179**, L41 (1987).
[70] P. Riviere, A. Salin, and F. Martín, J. Chem. Phys. **124**, 084706 (2006).
[71] C. Díaz, H. F. Busnengo, F. Martín, and A. Salin, J. Chem. Phys. **118**, 2886 (2003).
[72] H. F. Busnengo, W. Dong, P. Sautet, and A. Salin, Phys. Rev. Lett. **87**, 127601 (2001).
[73] D. Farías, C. Díaz, P. Riviere, H. F. Busnengo, P. Nieto, M. F. Somers, G. J. Kroes, A. Salin, and F. Martín, Phys. Rev. Lett. **93**, 246104 (2004).
[74] L. Bonnet and J. C. Rayez, Chem. Phys. Lett. **277**, 183 (1997).